Electrospun nanomaterials for ultrasensitive sensors

Increasing demands for ever more sensitive sensors for global environmental monitoring, food inspection and medical diagnostics have led to an upsurge of interests in nanostructured materials such as nanofibers and nanowebs. Electrospinning exhibits the unique ability to produce diverse forms of fibrous assemblies. The remarkable specific surface area and high porosity bring electrospun nanomaterials highly attractive to ultrasensitive sensors and increasing importance in other nanotechnological applications. In this review, we summarize recent progress in developments of the electrospun nanomaterials with applications in some predominant sensing approaches such as acoustic wave, resistive, photoelectric, optical, amperometric, and so on, illustrate with examples how they work, and discuss their intrinsic fundamentals and optimization designs. We are expecting the review to pave the way for developing more sensitive and selective nanosensors.

Bin Ding[a,b,*], Moran Wang[c,d,*], Xianfeng Wang[a,b], Jianyong Yu[b], Gang Sun[a]

[a] State Key Laboratory for Modification of Chemical Fibers and Polymer Materials, College of Materials Science and Engineering, Donghua University, Shanghai 201620, China

[b] Nanomaterials Research Center, Modern Textile Institute, Donghua University, Shanghai 200051, China

[c] Earth and Environmental Sciences Division, Los Alamos National Laboratory, Los Alamos, NM 87545, USA

[d] Physics of Condense Matter & Complex System, Theoretical Division, Los Alamos National Laboratory, Los Alamos, New Mexico 87545, USA

*E-mail: binding@dhu.edu.cn (BD) and mwang@lanl.gov (MW)

Compared with other methods of fiber preparation like drawing, template synthesis, self-assembly, phase separation, etc., electrospinning has emerged as a versatile and cost-effective method for producing long continuous fibers with diameters ranging from several micrometers down to a few nanometers by applying a high voltage on a polymer solution or melt[1]. In 1934, Formhals[2] described the operation of electrospinning in a US patent for the first time; but only since 1990s it has gained substantial attention. The process attracted rapidly growing interests in the past two decades triggered by potential

applications of nanofibers in the nanoscience and nanotechnology. Several research groups, especially the Reneker group, have revived interest in this technology, have shown the possibility to electrospin a wide variety of polymeric fibers[3,4]. A number of review articles have been published recently which provide an insight into the most prominent aspects of electrospinning[5-7].

In a typical electrospinning process, the surface of a hemispherical liquid drop suspended in equilibrium at the tip of a capillary will be distorted into a conical shape in the presence of an external electric field[8]. When the electric field is sufficiently strong, charges on the droplet surface will overcome the surface tension to induce the formation of a liquid jet that is subsequently accelerated toward a grounded collector. For low viscosity liquids, the jet breaks into droplets because of the longitudinal Rayleigh instability which is known as electrospraying, and used to obtain aerosols composed of sub-micrometer droplets with a narrow distribution[3]. For high viscosity liquids, such as polymer solutions or melts, the liquid travels in the form of a jet to the grounded target instead of breaking up. The transverse instability or spraying of the jet into two or more smaller jets is observed due to the radial charge repulsion[9]. As the solvent

is evaporating, this liquid jet is stretched to many times its original length to produce continuous, ultrathin fibers of the polymer. This process is termed 'electrospinning', and it produces polymer fibers with diameters of sub-micrometer scale[10]. These porous three-dimensional (3D) membranes assembled by electrospun fibers are featured with large specific surface area, high porosity, and good interconnectivity, which makes electrospun nanomaterials highly attractive to different applications ranging from filtration, sensors, drug delivery platforms, tissue engineering, and so on[5,6].

Nanofibers and nanowebs
Nanofibers
Electrospun nanofibers are featured with very small diameters, extremely long length, large surface area per unit mass and small pore size. Various materials such as polymers, ceramics and carbon can be used to electrospin uniform fibers with well-controlled sizes, compositions, and morphologies[11]. Different nanofiber morphologies can be obtained via control of the processing conditions to produce beaded as well as smooth and ribbon structures (Fig. 1a-c). Recent studies have demonstrated that this technique can also produce
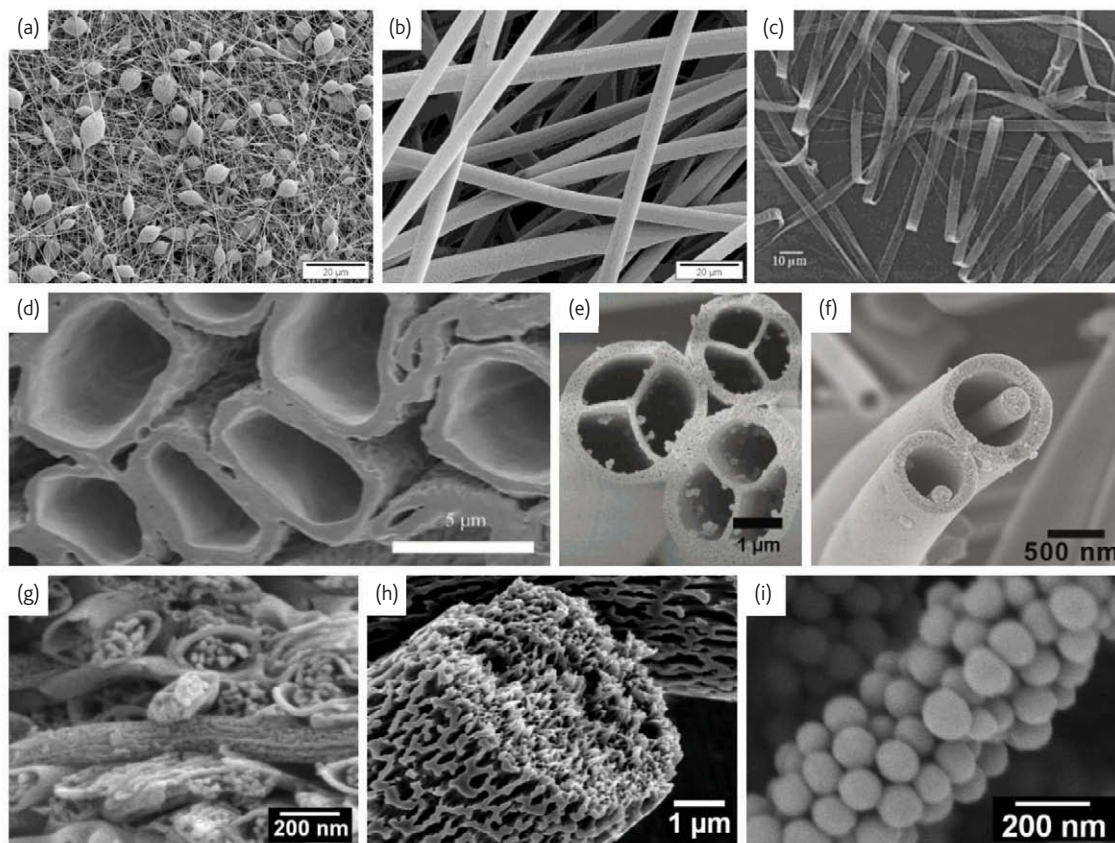

Fig. 1 Different morphologies of electrospun fibers: (a) beaded; (b) smooth (Reprinted with permission from[79]. © 2010 American Chemical Society.); (c) ribbon (Reprinted with permission from[87]. © 2001 Wiley.); (d) hollow (Reprinted with permission from[12]. © 2007 Wiley.); (e) multichannel tubular (Reprinted with permission from[13]. © 2007 American Chemical Society.); (f) nanowire-in-microtube (Reprinted with permission from[14]. © 2010 American Chemical Society.); (g) multi-core cable-like (Reprinted with permission from[15]. © 2007 IOP Publishing Ltd.) and (h,i) porous[16] fibers.
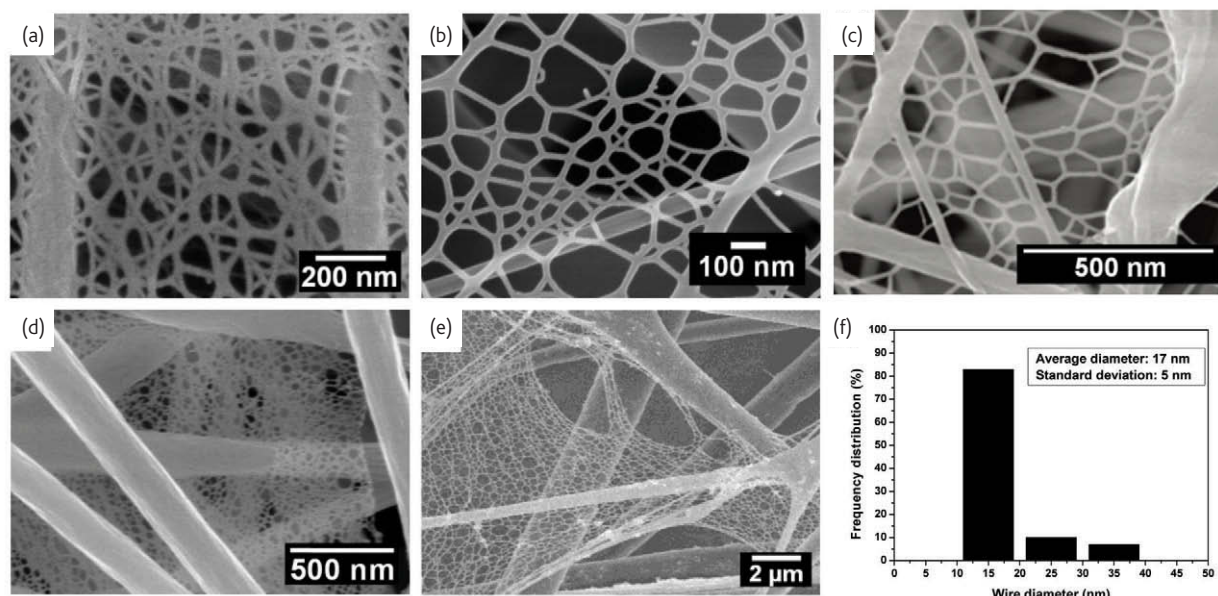
Fig.2 Nanowebs of various polymer systems: (a) SEM image of nylon-6 fibers formed in formic acid with a concentration of 20 wt%, voltage of 25 kV, spinning distance of 15 cm and relative humidity of 20%.(Reprinted with permission from[21]. © 2006 IOP Publishing Ltd.) (b) FE-SEM image of PAA nanowebs formed in a 7 wt% PAA solution with the cosolvent of ethanol and formic acid. (Reprinted with permission from[22]. © 2010 IOP Publishing Ltd.) (c) FE-SEM image of a polymerized PAA/nylon-6 mat. (Reprinted with permission from[24]. © 2009 American Chemical Society.) (d) FE-SEM image of composite PVA/ZnO nanowebs. (Reprinted with permission from[23]. © 2008 Elsevier Ltd.) (e) FE-SEM image of composite PVA/SiO$_2$ nanowebs. (f) Histogram showing the diameter distribution of nanowires shown in (a).

nanofibers with core-sheath or hollow[12], multichannel tubular[13], nanowire-in-microtube[14], multi-core cable-like[15] and porous[16-18] structures (Fig. 1d-i).

In comparison with other one-dimensional (1D) nanostructures such as nanorods and nanotubes, nanofibers are continuous, which possess them with high axial strength combined with extreme flexibility. Therefore the membranes assembled by electrospun nanofibers have excellent structural mechanical properties. Meanwhile, multiple extra functions can be incorporated into electrospun nanofibers to broaden their significances in applications. These include not only textile, ultrafiltration, tissue engineering, catalysis and mechanical reinforcement applications but extend to the fabrication of sensors, solar cells and other types of devices[15,19].

Nanowebs

The desires for ever higher specific surface area and porosity have pushed people to improve the electrospinning technique. An ideal fiber diameter is below 20 nm for optimal performances[20], however an electrospun fiber from the traditional process typically have a diameter in the range 100-500 nm. The objective is a robust method for manufacturing extremely small nanofibers in large quantities and with a uniform size. Recently, the novel two-dimensional (2D) nanowebs were generated in 3D fibrous mats by optimizing processing parameters in electrospinning[21]. The electrospun fibers act as a support for the 'fishnet-like' nanowebs comprising interlinked 1D nanowires (Fig. 2a-e). The nanowire diameter distribution of nylon-6

nanowebs is shown in Fig. 2f. The major range (over 80%) of nanowire diameters was 10-20 nm with a mean at 17 nm and a standard deviation of 5 nm. The mean diameter of the nanowires contained in typical nanowebs is about one order of magnitude less than that of conventional electrospun fibers. To date, various nanowebs have been successfully prepared using different polymer systems such as nylon-6[21], polyacrylic acid (PAA)[21,22], poly(vinyl alcohol) (PVA)[23] and PAA/nylon-6[24] (Fig. 2-e). The formation, morphology and area density of the nanowebs in electrospun fibrous membranes are strongly affected by the applied voltage, relative humidity (RH), solvents, solution concentration and distance between the capillary tip and the collector.

Ultrasensitive sensors based on electrospun nanomaterials

In response to the imperative needs for more timely and reliable detections in environmental monitoring, food inspection and medical diagnostics, tremendous progresses have been made in the development of ultrasensitive sensors. Developments of electrospun nanomaterials, such as nanofibers and nanowebs, have offered opportunities to construct more efficient interfaces with electronic components whose size is comparable to that of molecules. People may benefit from the tiny size with some special size effects, such as quantization and single-molecule sensitivity. The relatively huge specific surface area and high porosity of electrospun nanomaterials have attracted significantly increasing attentions because these

Table 1 Types of electrospun nanomaterials based sensors.

Types	Materials	Array of fibers	Fiber diameter	Targets tested	Operating temperature (°C)	Detection limit
Acoustic wave	PVP/LiTaO$_3$[28]	Nonwoven	200-400 nm	H$_2$	RT	1250 ppm
	PAA-PVA[30]	Nonwoven	100-400 nm	NH$_3$	RT	50 ppm
	PAA[32]	Nonwoven	1-7 μm	NH$_3$	RT	130 ppb
	PEI-PVA[33]	Nonwoven	100-600 nm	H$_2$S	RT	500 ppb
	PAA[22]	Nonwoven	11-264 nm	H$_2$O	RT	6%
	PEI-PVA[34]	Nonwoven	0.04-1.8 μm	HCHO	RT	10 ppm
Resistive	TiO$_2$[19]	Nonwoven	200-500 nm	NO$_2$	150-400°C	500 ppb
	TiO$_2$[88]	Nonwoven	120-850 nm	CO, NO$_2$	300-400 C	50 ppb
	LiCl-TiO$_2$[40]	Nonwoven	150-260 nm	H$_2$O	RT	11%
	Mg^{2+},Na$^+$-TiO$_2$[89]	Nonwoven	200 nm	H$_2$O	RT	11%
	TiO$_2$-ZnO[83]	Nonwoven	~250 nm	O$_2$	300°C	5.1×10^{-3} Torr
	SnO$_2$[90]	Single Nonwoven	700 nm	H$_2$O	RT	No data
	SnO$_2$[46]	Nonwoven	~100 nm	C$_2$H$_5$OH	330°C	10 ppb
	SnO$_2$[39]	Nonwoven	80-160 nm	Toluene	350°C	10 ppm
	MWCNT/SnO$_2$[91]	Nonwoven	300-800 nm	CO	RT	47 ppm
	ZnO-SnO$_2$[45]	Nonwoven	100-150 nm	C$_2$H$_5$OH	300°C	3 ppm
	Fe-SnO$_2$[92]	Nonwoven	60-150 nm	C$_2$H$_5$OH	300°C	10 ppm
	KCl-SnO$_2$[48]	Nonwoven	100-200 nm	H$_2$O	RT	11%
	ZnO-SnO$_2$[47]	Nonwoven	100-200 nm	Toluene	200-400°C	10 ppm
	α-Fe$_2$O$_3$[93]	Nonwoven	150-280 nm	C$_2$H$_5$OH	200-400°C	100 ppm
	ZnO[94]	Nonwoven	80-235 nm	C$_2$H$_5$OH	220°C	10 ppm
	Ag-In$_2$O$_3$[95]	Nonwoven	60-130 nm	HCHO	115°C	5 ppm
	PPy-TiO$_2$/ZnO[84]	Nonwoven	100 nm	NH$_3$	RT	60 ppb
	Pt/In$_2$O$_3$[96]	Nonwoven	60-100 nm	H$_2$S	140-300°C	50 ppm
	WO$_3$[97]	Nonwoven	20-140 nm	NH$_3$	350°C	50 ppm
	SrTi$_0$ Fe$_{0.2}$O$_{3-\delta}$[98]	Nonwoven	~100 nm	CH$_3$OH	400°C	5 ppm
	TiO$_2$-PEDOT[36]	Nonwoven	72-108 nm	NO$_2$	RT	7 ppb
				NH$_3$	RT	675 ppb
	HCSA-PANI/ PEO[50]	Single	100-500 nm	NH$_3$	RT	500 ppb
	PANI/PVP[53]	Nonwoven	1-10 μm	NO$_2$	RT	1 ppm
	PDPA-PMMA[55]	Nonwoven	~400 nm	NH$_3$	RT	1 ppm
	PANI[51]	Nonwoven	0.3-1.5 μm	Amines	RT	100 ppm
	PMMA-PANI[52]	Nonwoven	250-600 nm	(C$_2$H$_5$)$_3$N	RT	20 ppm
	HCSA-PANI[54]	Single	20-150 nm	Alcohols	RT	No data
	PEO-PANI[99]	Nonwoven	250-500 nm	H$_2$O	RT	22%
	HCSA-POT/PS[56]	Nonwoven	0.2-1.9 μm	H$_2$O	RT	No data
	MWCNT/nylon[57]	Nonwoven	110-140 nm	VOCs	RT	No data
	CB-PECH, PEO, PIB,PVP[100]	Oriented	~3 μm	CH$_3$OH	RT	1000 ppm
				C$_5$H$_{10}$Cl$_2$		5 ppm
				C$_6$H$_5$CH$_3$		250 ppm
				C$_2$HCl$_3$		500 ppm

Abbreviations in Table 1: PAA (polyacrylic acid); PVA (polyvinyl alcohol); PEI (polyethyleneimine); HCSA (10-camphorsulfonic acid); PANI (polyaniline); PEO (polyethylene oxide); PDPA (polydiphenylamine); PMMA (polymethyl methacrylate); POT (poly(o-toluidine)); PS (polystyrene); MWCNT (multi-walled carbon nano-tube); PPy (polypyrrole); CB (carbon black); PECH (polyepichlorohydrin); PIB (polyisobutylene); PVP (polyvinyl pyrrolidone); PEDOT (poly(3,4-ethylenedioxythiophene)); PM (poly(pyrene methanol)); PAN (polyacrylonitrile); DNT (2,4-dinitrotoluene); PCDA (10,12-Pentacosadiynoic acid); α-CD (α-cyclodextrin); GOx (glucose oxidase); PVdF (poly(vinylidene fluoride); PAPBA poly(aminophenylboronic acid)); NiCFP (Ni nanoparticle-loaded carbon nanofiber paste); PCNFs (Pd (IV)-doped CuO oxide composite nanofibers); VOC (volatile organic compound); H$_2$O$_2$ (hydrogen peroxide); RT (room temperature).

Table 1 continued.

Types	Materials	Array of fibers	Fiber diameter	Targets tested	Operating temperature (°C)	Detection limit
Photoelectric	Au/SiO$_2$[60]	Nonwoven	130-170 nm	Wavelength	RT	No data
	Co-ZnO[101]	Nonwoven	50-400 nm	O$_2$	RT	0.32 Torr
	GaN[61]	Nonwoven	32-48 nm	Wavelength	RT	No data
Optical	PAA-PM[62]	Nonwoven	100-400 nm	Fe^{3+}, Hg^{2+}, DNT	RT	No data
	Oxides-PAN[65]	Nonwoven	50-200 nm	CO$_2$	RT	700 ppm
	PCDA[64]	Single	3 μm	α-CD	30°C	No data
Amperometric	GOx/PVA[71]	Nonwoven	70-250 nm	Glucose	RT	0.05 mM
	PVdF/PAPBA[76]	Nonwoven	~150 nm	Glucose	RT	1 mM
	NiCFP[73]	Nonwoven	200-400 nm	Glucose	RT	1 μM
	PCNFs[75]	Nonwoven	90-140 nm	Glucose	RT	190μM
	CuO[74]	Nonwoven	170 nm	Glucose	RT	80 μM
	Hemoglobin[77]	Nonwoven	~2.5 μm	H$_2$O$_2$	RT	0.61 μM
				Nitrite		0.47 μM
	PVP/urease[78]	Nonwoven	~100 nm	Urea	RT	0.5 mM

Abbreviations in Table 1: PAA (polyacrylic acid); PVA (polyvinyl alcohol); PEI (polyethyleneimine); HCSA (10-camphorsulfonic acid); PANI (polyaniline); PEO (polyethylene oxide); PDPA (polydiphenylamine); PMMA (polymethyl methacrylate); POT (poly(o-toluidine)); PS (polystyrene); MWCNT (multi-walled carbon nano-tube); PPy (polypyrrole); CB (carbon black); PECH (polyepichlorohydrin); PIB (polyisobutylene); PVP (polyvinyl pyrrolidone); PEDOT (poly(3,4-ethylenedioxythiophene)); PM (poly(pyrene methanol)); PAN (polyacrylonitrile); DNT (2,4-dinitrotoluene); PCDA (10,12-Pentacosadiynoic acid); α-CD (α-cyclodextrin); GOx (glucose oxidase); PVdF (poly(vinylidene fluoride); PAPBA poly(aminophenylboronic acid)); NiCFP (Ni nanoparticle-loaded carbon nanofiber paste); PCNFs (Pd (IV)-doped CuO oxide composite nanofibers); VOC (volatile organic compound); H$_2$O$_2$ (hydrogen peroxide); RT (room temperature).

properties meet ideally the desired requirements for ultrasensitive sensors. A survey of open publications related with 'electrospinning and sensor' in the past 10 years is given in Fig. 3. In this section, we review and introduce some recent progress and predominant developments of several sensing approaches, including acoustic wave, resistive, photoelectric, optical, and amperometric sensors. A comprehensive summary of sensors based on the electrospun nanomaterials is illustrated in Table 1.
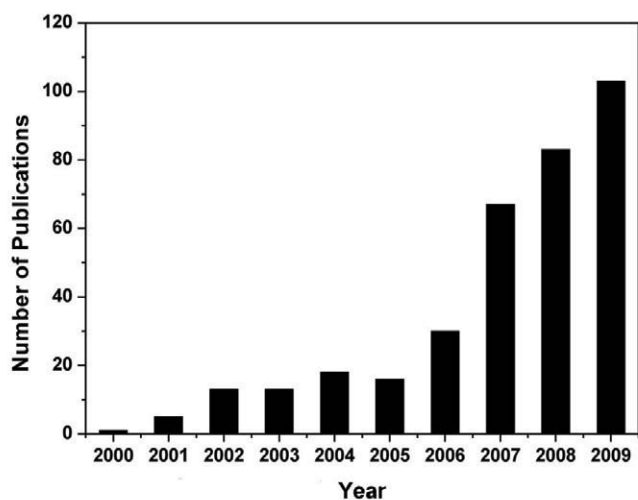

Fig. 3 Comparison of the annual number of scientific publications with the keyword ''electrospinning and sensor'', as provided by the search engine of SciFinder Scholar. For 2010, there are already 42 publications before May 30.

Acoustic wave sensors

Recently, there has been a growing attention toward developing surface acoustic wave (SAW) devices for gas sensing applications[25,26]. A more surface-confined acoustic wave can be obtained by depositing sensing layers onto the active area of the SAW device. The change in electrical conductivity or mass of the sensing layer perturbs the velocity of SAW due to mechanical and piezoelectric effects. Concentrated efforts have been focused on depositing nanostructured coatings on SAW *via* electrospray or electrospinning techniques to improve the sensor sensitivity[27,28]. For example, He *et al.*[28] demonstrated that a sensor for H$_2$ could be prepared by electrospinning deposition of poly(vinylpyrrolidone) (PVP)/LiTaO$_3$ composite nanofibers on the electrodes of SAW.

Quartz crystal microbalances (QCMs), one of the acoustic wave techniques was first developed in 1880 based on the piezoelectric effect[29]. The QCM as an analytical tool is able to detect very tiny mass changes of even less than a nanogram deposited on crystal surface. Recent efforts have been focused on the development of nanostructured coatings on QCM to improve sensor sensitivities[30,31]. Taking the advantages of large specific surface area, high porosity and good interconnectivity of the electrospun fibrous assemblies, NH$_3$[30,32], H$_2$S[33], formaldehyde[34] and moisture[22] have been successfully detected under more challenging conditions at the room temperature in flow-type (Fig. 4a) or static-type gas testing systems (Fig. 4c) by measuring the resonance frequency shifts of QCM caused by the additional mass loading. The PAA nanofibers coated QCM sensors exhibited ultra-high
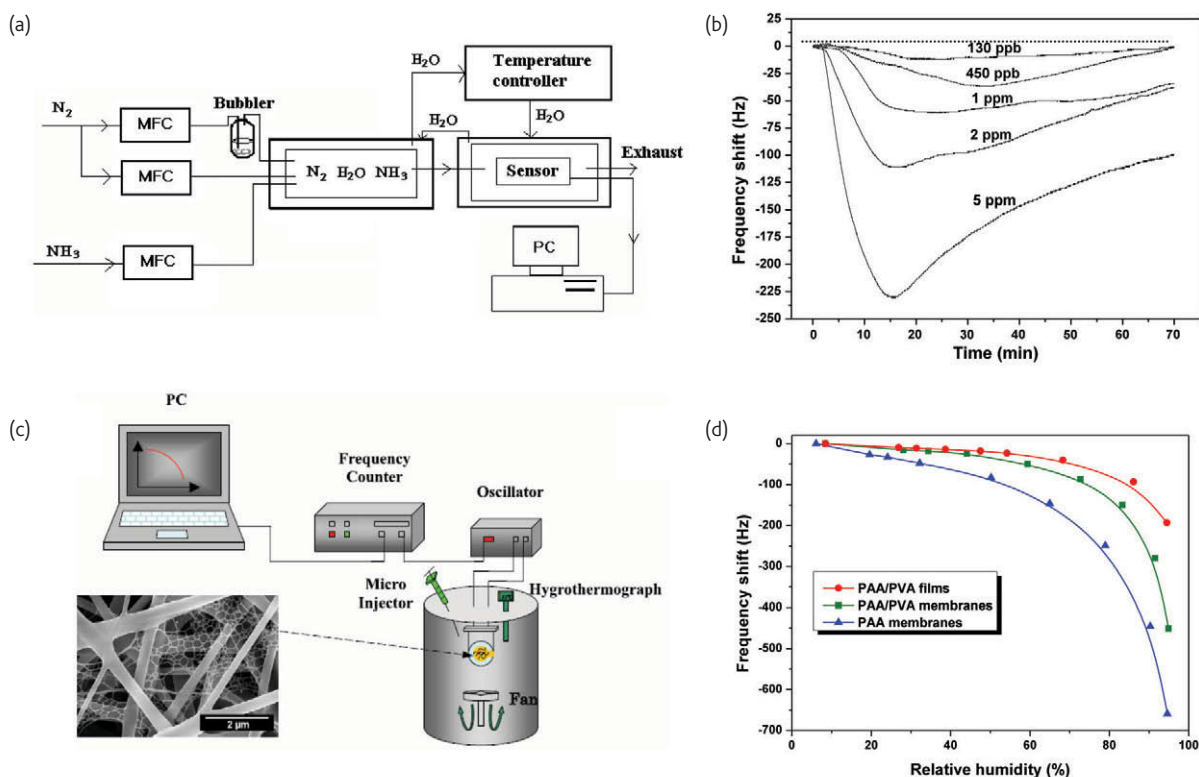
Fig. 4 (a) Schematic of a flow-type gas testing system for NH$_3$ detection. (b)Response of the PAA fibrous membrane coated QCM sensors exposed to various concentrations of NH$_3$. (Reprinted with permission from[32]. © 2005 Elsevier Ltd.) (c) Schematic diagram of a static-type testing system for humidity detection. (d) Frequency shifts of polyelectrolyte coated QCM sensors as a function of the relative humidity. (Reprinted with permission from[22]. © 2010 IOP Publishing Ltd.)

sensitivity towards very low concentrations of NH$_3$, such as 130 ppb at the RH of 40%[32] (Fig. 4b). Additionally, a humidity sensor was fabricated by electrospinning deposition a network of PAA nanowebs on a QCM[22]. The fibrous coatings produce a response increased by more than two orders of magnitude as RH increases from 6 to 95% (Fig. 4d). The sensitivity of the fibrous membranes coated QCM sensors was several times higher than that of the flat films coated QCM sensors. These experiments have demonstrated the possibility of using electrospinning technique to regulate structures of membrane for higher surface activity and gas sensitivity. More experiments using more complex arrangements and structures of fibers are expected to expand the capabilities of this platform in the future.

Resistive sensors

As well-known, one-dimensional nanostructured metal-oxide semiconductors (MOS) advance in facilitating fast mass transfer of the analyte molecules to and from the interaction region and requiring charge carriers to traverse any barriers introduced by molecular recognition events along the entire wire. Many attempts have been taken to prepare ultrasensitive resistive sensors to detect NH$_3$, H$_2$S, CO, NO$_2$, O$_2$, CO$_2$, moisture and volatile organic compounds vapors with new detection limits using electrospun nanofibers functionalized MOS such as TiO$_2$, ZnO, WO$_3$, MoO$_3$, SnO$_2$, In$_2$O$_3$ and ITO[35-39].

Among MOS, TiO$_2$ have been the most popular candidate used in ultrasensitive resistive sensors. Kim et al.[19] have demonstrated the use of nanofibers functionalized TiO$_2$ as detectors for NO$_2$. Li et al.[40] demonstrated the fabrication of LiCl-doped TiO$_2$ nanofibers via electrospinning as the humidity sensors (Fig. 5). They prepared a solution of tetrabutyltitanate, LiCl, and PVP in ethanol and acetic for electrospinning, followed by calcination to obtain TiO$_2$/LiCl composite nanofibers (Fig. 5a). The as-prepared humidity sensor based on the LiCl-doped TiO$_2$ nanofibers exhibited greatly improved sensitivity compared to the pure TiO$_2$ nanofibers. Additionally, the composite nanofibers also exhibited an ultra-fast response and recovery behavior (Fig. 5b). Recently, SnO$_2$ nanostructures have also received much attention due to their high transparency, wide-bandgap semi-conductivity, and huge magnetooptic and chemical-sensing effects[41,42]. SnO$_2$ nanofibers exhibit an electrical resistance sensitive to harmful chemical gases or vapors, such as ammonia[43], methanol[44], ethanol[45,46], toluene[47] and moisture[48]. Ultrasensitive detection of analytes in air with semiconducting metal-oxide resistive nanofiber chemiresistors provided one of the most impressive demonstrations of nanoelectronic sensing to date and has clear implications for the future environmental pollution monitoring devices. Given the distinct properties of these wide-band semiconductor materials possess, it is easy to envision them as a basis for a future generation of
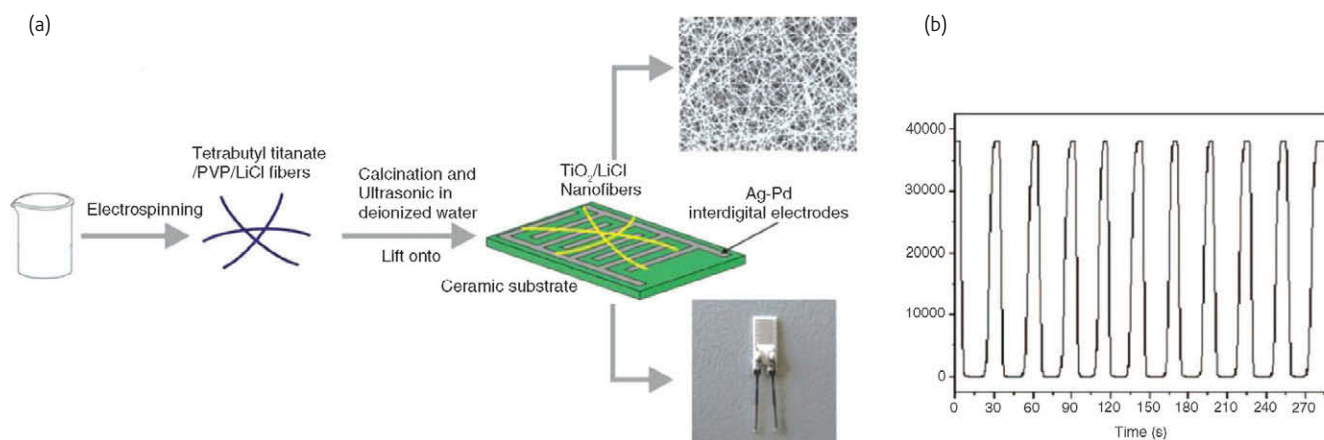
Fig. 5 (a) Schematic diagram of the processing steps used to fabricate LiCl doped TiO$_2$ nanofiber mats on Al$_2$O$_3$ substrate with interdigitated Pt electrode arrays. (b)Response and recovery characteristic curves based on the product containing 30.0% LiCl-doped TiO$_2$ nanofibers for 10 cycles. (Reprinted with permission from[40]. © 2008 American Chemical Society.)

non-intrusive highly efficient and extremely sensitive multifunctional electronic devices.

Besides the MOS sensing architectures, conducting polymer-based nanostructured materials have also been utilized extensively in resistive sensors because of their high surface areas, chemical specificities, tunable conductivities, material flexibilities and easy processing. Various kinds of conducting polymers, such as polyaniline (PANI), poly(diphenylamine) (PDPA), polypyrrole (PPy), and polythiophene, have been used in various applications including metallic interconnects in circuits, chemical sensors and electromagnetic radiation shielding[49]. Among the family of conducting polymers, PANI is one of most attractive materials for sensing applications. Over the past a few years, various PANI-based electrospun nanomaterials such as individual PANI/poly(ethylene oxide) (PEO) nanowires[50], PANI nanotubes[51], coaxial PANI/polymethacrylate (PMMA) composite nanofibers[52], leucoemeraldine-based PANI/PVP composite films[53] and 10-camphorsulfonic acid (HCSA) doped PANI nanofibers[54] have been explored as sensing materials for various gas detection. Additionally, other conducting composite electrospun fibers, such as PDPA/PMMA[55], HCSA doped poly(o-toluidine)/polystyrene[56] and multiwall carbon nanotube (MWCNT) doped nylon[57], were also fabricated as sensing materials to detect ammonia, alcohols, moisture, hexane, acetone, ethyl acetate, dichloromethane, trichloromethane, tetrahydrofuran and toluene vapors by measuring the resistance changes of fibers.

Photoelectric sensors

Metallic nanoparticles encapsulated into dielectric matrices are considered to have practical applications in optical and electronic devices owing to their enhanced third-order nonlinear susceptibility, especially near the surface-plasmon-resonance (SPR) frequency[58]. The enhancement of photoresponse behaviors in the hybrid nanowire arising from the excitation of the surface plasmon is attributed to the generation of hot electrons owing to the decay of surface plasmon polaritons[59]. Recently, Shi and coworkers[60] have developed a method to fabricate Au nanoparticles (AuNPs) embedded silica nanofibers via electrospinning and thermal decomposition of hybrid nanofibers, which exhibited an obvious photoelectric response under the illumination (Fig. 6a). Upon illumination, the hybrid peapod nanofibers presented a wavelength-dependent photoelectric current response. In particular, the current photoresponse reached a maximum value under illumination at a wavelength of 550 nm, which was close to the SPR absorption band of the AuNPs nanofibers (Fig. 6b). These results showed the potential of using gold nanopeapodded silica nanowires as wavelength-controlled optical nanoswitches.

Another type of photoelectric sensor based on 1D nanosized GaN has been developed recently. Considering the distinguished optical and electric performance, electrospun GaN nanofibers are suitable for ultraviolet photodetection applications. Pan and coworkers[61] demonstrated that electrospun GaN nanofibers were promising candidates for easily assembled high-performance UV photodetectors (Fig. 6c). The photoconductance of an electrospun GaN nanofiber increases by 830 times compared with single crystalline GaN nanowires when UV was on. This high sensitivity can be attributed to the polycrystalline structure and rough surfaces of GaN nanofibers, which lead to a high surface area-to-volume ratio, and subsequently result in more photogenerated carriers compared with a smooth GaN nanowire. Besides high sensitivity, the electrospun GaN nanofiber UV sensor also showed advantages in response speed and reversibility as seen in Fig. 6d.

Optical sensors

Optical fiber sensors have many advantages than the traditional types of sensors such as the absences of electromagnetic interference in sensing and electric contacts in the probe, and multiplexity on a single
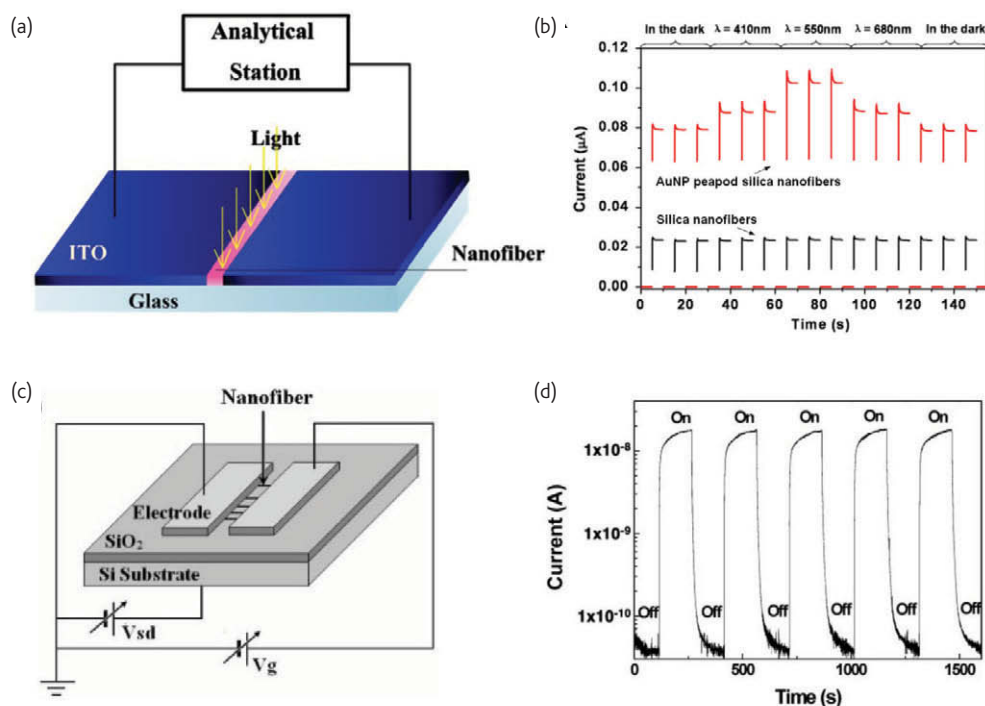
Fig. 6 (a) A schematic of the microreactor for photoelectric response measurements. (b) Photoelectric response measurements of the room-temperature current response as a function of time of light illumination for pure silica nanofibers and AuNPs peapod silica nanofibers. (Reprinted with permission from[60]. © 2009 Elsevier Ltd.) (c) Schematic view of the GaN nanofiber UV photodetector configuration. The source and drain contacts are silver strips, and a heavily doped p-type Si substrate serves as the back gate. (d) Conductance response of a GaN nanofiber upon pulsed illumination from a 254 nm wavelength UV light with a power density of 3 mW cm^{-2}. (Reprinted with permission from[61]. © 2009 Wiley.)

net work. Electrospun optical sensors can be grouped into two general types: (i) the quenching-based fluorescent optical sensors and (ii) the Fourier transform infrared (FTIR) spectroscopy optical sensors.

The pioneering work of Wang and coworkers[62] have successfully developed nanofibrous PAA-pyrene methanol membranes optical sensors for metal ion (Fe^{3+} or Hg^{2+}) and 2,4-dinitrotoluene detection using the electrospinning technique. Additionally, Wang et al.[63] reported a optical sensor by layer-by-layer (LBL) assembling fluorescent probes on to electrospun cellulose acetate nanofibers, which showed fluorescence quenching upon exposure to even an extremely low concentration (ppb) of methyl viologen cytochrome in aqueous solutions (Fig. 7a). Owing to the intriguing stress-induced chromic transition and nonlinear optical properties, polydiacetylene supramolecules (PDAs) have been extensively investigated as potential chemosensors and photonic materials. Chae et al.[64] have demonstrated the feasibility of PDA-embedded electrospun microfibers as potential sensor materials by detecting the fluorescence generation upon specific ligand-receptor interactions (Fig. 7b-d). Incubation of the porous PMMA microfibers, containing embedded polymerized PCDA, in an α-cyclodextrin (α-CD) solution (10 mM) resulted in the generation of red fluorescence (Fig. 7d), however, much weaker fluorescence signals arose from fibers treated with β- and γ-CD.

FTIR spectroscopy is another popular optical method to study the interaction of electromagnetic radiation in the infrared region with chemical compounds. Different functional groups within a compound absorb radiation at different frequencies and yield unique infrared absorbance spectra. An absorbance band may be characterized by a central wave number and the associated maximum intensity. The large band width (400-4500 cm^{-1}) and the distinct absorbance bands render the FTIR technology suitable for sensor applications. Hahn et al.[65] first utilized the electrospun polyacrylonitrile/Fe_2O_3 fiber mats as optical sensor in conjunction with FTIR spectroscopy to detect CO_2, which showed enhanced intensity by about 140% compared with flat films when exposed to 2000 ppm of CO_2.

Amperometric sensors

The past several decades have witnessed the big progress on fabricating sensitive devices for fast and reliable monitoring glucose and carbohydrates driven by their practical applications in treating and controlling diabetes[66]. Various techniques such as chemiluminescence[67], chromatography[68] and electrochemistry[69] were applied in glucose determination, in which, electrochemical methods, especially amperometry, have been proved to be a powerful approach and attracted much attention. Up to now, most amperometric sensors based on electrospun nanomaterials were used to detect glucose. Among those devices, amperometric glucose biosensors with glucose oxidase (GO_x) and without GO_x have been an intensively research area because a low detection limit can be achieved easily.
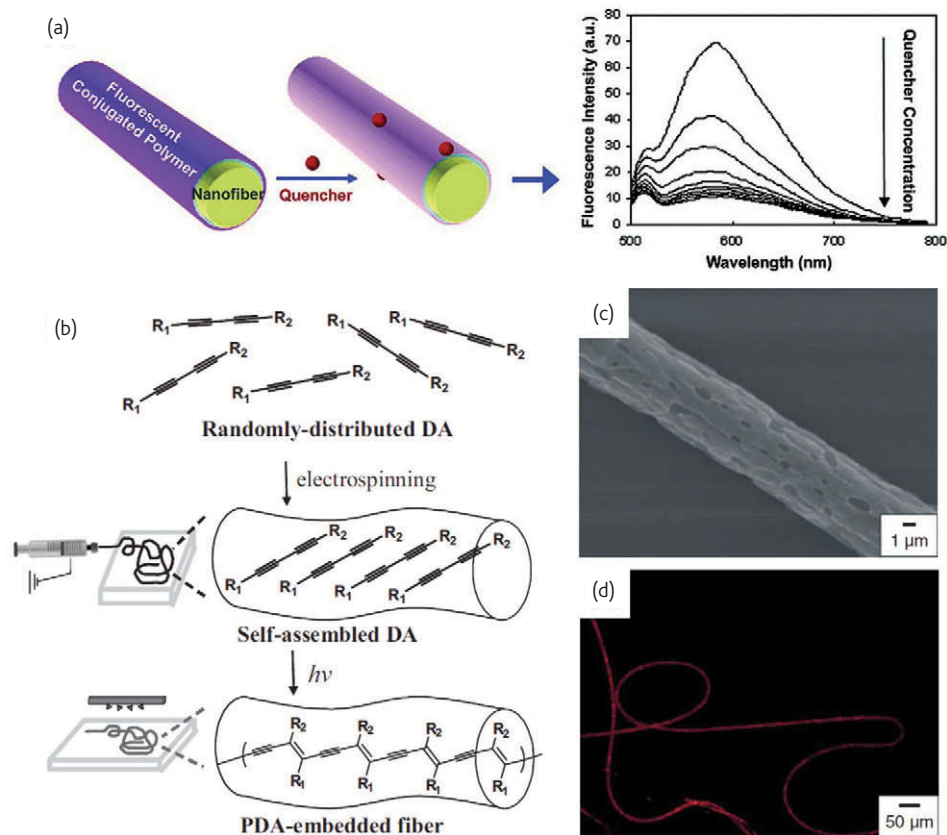
Fig. 7 (a) Assembling fluorescent probes on to electrospun CA nanofibers and Fluorescence emission spectra of the sensing film with varying quencher concentration. (Reprinted with permission from[63]. © 2004 American Chemical Society.) (b) Schematic representation of the preparation of polymer microfibers-embedded with PDAs by using the electrospinning technique, followed by irradiation with UV light (254 nm). (c) SEM image of an electrospun PCDA-embedded PMMA fiber after photopolymerization. (d) Fluorescence microscopy image of the polymer fiber after treatment with a 10 mM α-cyclodextrin solution. (Reprinted with permission from[64]. © 2007 Wiley.)

Since the first work was proposed on enzymatic electrode, electrochemical biosensors with the GO_x binding to the transducers have played a leading role in this direction. Considering the immobilization of GO_x, various carbon-based nanoscaled materials such as carbon nanofiber, carbon nanotube, carbon nanohorn, mesoporous carbon and graphite nanoplatelet were explored as immobilization matrix due to their unique electronic and mechanical properties. Wang et al.[70] explored the application of carbon nanotube-filled electrospun nanofibrous poly(acrylonitrile-*co*-acrylic acid) membranes in glucose biosensor (Fig. 8a-b), in which fast response and low detection limit were achieved. Apart from these carbon-based nanoscaled immobilization matrix, Ren et al.[71] have developed an amperometric biosensor by electrospinning deposition of nanofibrous GO_x/PVA membranes as sensitive coatings on the surface of the Au electrode. The electrospinning technique makes it convenient and efficient to prepare the enzymatic electrode for biosensors.

Good selectivity and high sensitivity were obtained with these enzymatic sensors, while inevitable drawbacks such as the chemical and thermal instabilities originated from the intrinsic nature of enzymes as well as the tedious fabrication procedures may limit their

analytical applications[72]. Most enzymeless electrochemical glucose sensors rely on the properties of electrode materials, on which glucose is oxidized directly. With the great development of nanotechnology, various electrospun nanomaterials such as Ni nanoparticle-loaded carbon nanofibers (NiCF)[73], copper oxide nanofibers[74], Pd(IV)-doped copper oxide composite nanofibers[75] and poly(vinylidene fluoride)/poly(aminophenylboronic acid) composite nanofibrous membranes[76] were explored as the candidates in the hope of developing effective enzyme-free sensors. As an example, the amperometric responses of the NiCF paste electrode are shown in Fig. 8c. As indicated, fast response with 95% of the steady-state current achieved within 5 seconds could be observed, and the limit of detection was 1 μM. The good analytical performance and straightforward preparation method made enzymeless electrode material promising for the development of effective glucose sensor.

Apart from these predominant glucose sensors, many research groups have investigated the application of biomaterials modified amperometric devices to detect hydrogen peroxide (H_2O_2), nitrite, urea, and so on, which further extend the scope of amperometric biosensors. For instance, Ding et al.[77] have developed an amperometric
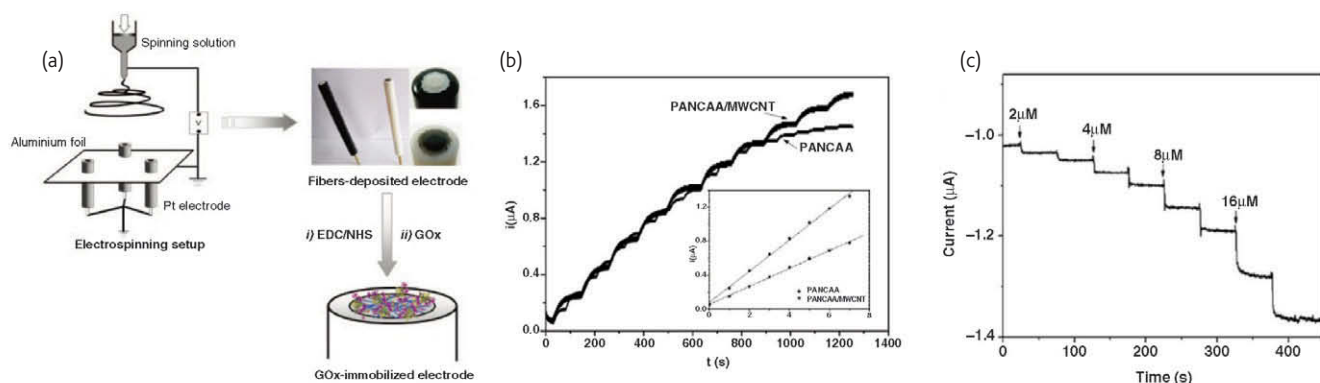
Fig. 8 (a) Schematic illustration of electrospinning for GOx electrode. (b) Chronoampeometric curves with various glucose concentrations on the PANCAA and MWCNT-filled PANCAA (PANCAA/MWCNT) nanofibrous membrane deposited electrodes. The glucose was added at every interval. The inset shows the plots of the steady-state limiting current against the concentration of glucose. (Reprinted with permission from[70]. © 2009 American Chemical Society.) (c) Current-time responses of the NiCFP electrode upon successive addition of glucose at low concentrations. (Reprinted with permission from[73]. © 2009 Elsevier Ltd.)

biosensor by electrospinning deposition of hemoglobin microbelts as sensitive coatings on the surface of the glassy carbon electrode. The hemoglobin microbelts based amperometric biosensor showed a fast response to the analytes and had excellent detection limits of 0.61 μM for H_2O_2 and 0.47 μM for nitrite. As is known to all, urea levels are vital in medical diagnosis, environmental and bioindustrial analysis. Recently, researchers at the University of New York have demonstrated that electrospun PVP/urease composite nanofibers had great potential as a urea biosensor[78]. These nanocomposite materials exhibited high electric conductivity and accelerated the electron transfer, which in turn greatly enhanced the sensor sensitivity.

Optimization analysis of sensor performance
Specific surface area and fiber diameter
Growing efforts have been focused on developments of nanostructured materials to achieve higher surface-to-volume ratios and lower cross-section areas, which lead to more effective performances of electrochemical detectors such as mass transport, electric charge transport and signal to noise current ratios. Various hyperfine nanostructures, such as porous, hollow and core-sheath structures, can be obtained via regulating the parameters of electrospinning process or solution properties.

Porous nanofibers can be produced by different ways, for instances via polymer blends, solvents caused phase separations, and spinning onto very cold substrates such as liquid nitrogen or on different collectors[5,79,80]. Nanofibers with porous structures can also be produced from bicomponent systems by calcination or porogen treatment[17]. Zhang and coworkers[81] have demonstrated the feasibility of preparing porous SnO_2 fibers through electrospinning of PVA/SnCl$_4$·5H$_2$O composite and oxygen plasma etching. The highly porous SnO_2 fibers composing of nano-size fibrils outperformed the conventional bulk films in both sensitivity and response time to ethanol.

To obtain hollow or core-shell fibers, an electrospun nanofiber serves as a template onto which a second material is deposited as shell either from solution or melt, via layer-by-layer techniques, or from the vapor phase[11,82]. Especially for hollow fibers, the core fiber can be removed by thermal decomposition, selective solvents, or by biodegradation. The internal surface of the hollow fibers is structured in this case by the surface topology of the template fibers. Choi et al.[37] demonstrated that hollow ZnO fibers (Fig. 9a) enhanced the sensitivity to NO_2 compared with the reference ZnO thin film specimens (Fig. 9b). Park et al.[83] and Wang et al.[36] also described that an sensitivity increase was observed with the fabrication of TiO_2-ZnO core-shell and TiO_2-poly (3,4-ethylenedioxythiophene) structured nanofibers. These works have proved the possibility to form numerous interesting inorganic tubular structures with homogenous wall thickness and secondary structure.

The manufacturing of structured yet compact polymer fibers with diameters from submicrometer to 10 nm meets with considerable interests for various kinds of applications. The reduction of diameter into nanometers gives rise to a set of favorable properties, including increase of surface-to-volume ratio, unique electronic properties, and simple integration with two-terminal microcircuits, which will further enhance the sensitivity of the sensor. Craighead and coworkers[50] investigated the diameter-dependent response of single PANI upon exposure to NH_3. The PANI nanowires with two different diameters (335 and 490 nm) were fabricated and their sensitive properties were examined. As a result, the electrical response of single PANI nanowire sensors depended on the vapor concentration as well as the nanowire diameter. Both the response time and the sensitivity were greatly improved with the decrease of diameter. Therefore, a smaller diameter leads to a faster response due to more rapid diffusion of gas molecules through the nanowire.

Membrane thickness
With different sensing mechanisms, the influence of membrane thickness on sensor sensitivity might be different. With regard to mass
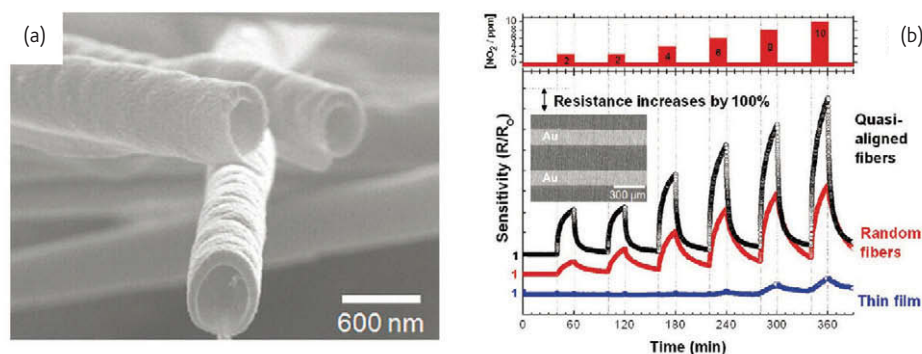
Fig. 9 (a) SEM micrograph of hollow ZnO fibers after calcination at 500 °C. (b) The resistance response during cyclic exposure to increasing NO_2 concentrations at 350 °C of sensors comprising a network of nonaligned or quasi-aligned hollow ZnO fibers and a reference ZnO thin film sensor. The NO_2 gas concentration profile is shown on top. The inset shows a SEM micrograph of quasi-aligned fibers on an interdigitated alumina substrate. (Reprinted with permission from[37]. © 2009 American Chemical Society.)

sensing technique, a thicker nanofibrous membrane has a larger sensing area and vacant volume in which more analytes can be absorbed and diffuse into the membranes. We demonstrated that the nanofibrous PAA membranes coated QCM sensors with a larger coating load exhibited a larger frequency response for the same RH[22]. For resistive sensors, increased interaction of the analyte with the conduction channel is of importance, as the sensitivity and response time ultimately depend on the analyte transport to this region. It may be possible that a thicker semiconductor or conducting polymer layer could protect the conduction pathway from the deleterious effects of environment as well as analytes of interest. Wang et al.[84] demonstrated how ultrathin PPy membranes influenced the sensor characteristics. The high sensitivity and fast recovery time can be attributed to the ultrathin PPy-coating layer (~7 nm), in which the ultrathin PPy layer greatly reduces the diffusion resistance of NH_3. Nevertheless, the dependence of sensing performance on nanofibrous membranes thickness has not been clearly established for resistive sensors[85].

Conclusion

The past few years have witnessed significant progresses in applications of the electrospun nanomaterials, demonstrated by numbers of recent scientific publications on this area. Current research has focused on not only the theory and optimization of the electrospinning process, but also many specific aspects of electrospun nanomaterials such as structure formation, functionalization, potential implementation in devices and other applications[86]. Although most of these topics are of fundamental interest, they have been, for the most parts, studied only rudimentarily to date.

Essential studies, nevertheless, are still required and many challenges have to be faced. More experimental studies and theoretical modeling are required in order to achieve a better control over the size and morphology of electrospun fibers. In particular, nanofiber systems with ultrafine diameter less than 20 nm exhibit several fascinating characteristics such as extremely large specific surface area, high porosity and superior mechanical performance, which make them

optimal candidates for applications in ultrasensitive sensors as well as the ultra-fine filters to intercept viruses and bacteria such as influenza A (H1N1) virus, severe acute respiratory syndrome (SARS) virus, *Escherichia coli*, etc. Until now, thorough understanding the formation mechanisms of nanowebs has been an imperative challenge. Only after solving this challenge, we can successfully prepare more and better nanowebs with different polymers and precisely control the actual mechanics in the progress of electrospinning.

Preparation of sensing materials in form of nanostructures may significantly improve their performances in the existing devices or open the doors to new types of applications. For instance, the research on engineering the secondary structures (porous and core-sheath or hollow) of electrospun nanomaterials will provide a new platform for designing advanced electrode materials, catalyst supports, and sensing devices. However, integration of such nanomaterials into useful devices requires materials of well-controlled orientation, size, and other targeting characteristics as well as reproducibility locating them in specific positions and orientations. The ability to narrow the compatibility gap between sensing devices and nanomaterials, however, remains a major challenge in the field. Fortunately, several approaches have emerged that promise to bridge these gaps and realize the vision of upgraded nanosensors.

There is no doubt that electrospinning has become one of the most powerful techniques for preparing diverse nanostructured materials and highly sensitive sensors in the future. The combination of these diverse areas of research promises to yield revolutionary advances in environmental monitoring, food inspection and medical diagnostics through the creation of novel and powerful tools that enable direct, sensitive, and rapid analysis of chemical species. mt

Acknowledgments

REFERENCES

1. Maheshwari, S., and Chang, H. C., *Adv. Mater.* (2009) **21**, 349.
2. Formhals, A., *Process and Apparatus for Preparing Artificial Threads*, US Patent 1,975,504, (1934).
3. Reneker, D. H., and Chun, I., *Nanotechnology* (1996) **7**, 216.
4. Fong, H., *et al.*, *Polymer* (1999) **40**, 4585.
5. Li, D., and Xia, Y. N., *Adv. Mater.* (2004) **16**, 1151.
6. Greiner, A., and Wendorff, J. H., *Angew. Chem. Int. Ed.* (2007) **46**, 5670.
7. Ramakrishna, S., *et al.*, *Materials Today* (2006) **9**, 40.
8. Deitzel, J. M., *et al.*, *Polymer* (2001) **42**, 261.
9. Doshi, J., and Reneker, D. H., *J. Electrostatics* (1995) **35**, 151.
10. Dzenis, Y., *Science* (2004) **304**, 1917.
11. Li, D., *et al.*, *Small* (2005) **1**, 83.
12. Dror, Y., *et al.*, *Small* (2007) **3**, 1064.
13. Zhao, Y., *et al.*, *J. Am. Chem. Soc.* (2007) **129**, 764.
14. Chen, H. Y., *et al.*, *Langmuir* (2010) **26**, 11291.
15. Kokubo, H., *et al.*, *Nanotechnology* (2007) **18**, 165604.
16. Ding, B., *et al.*, *Nanotechnology Research: New Nanostructures, Nanotubes and Nanofibers, Nova Science Publishers, New York* (2008), 131
17. Kanehata, M., *et al.*, *Nanotechnology* (2007) **18**, 315602.
18. Wang, M. R., *et al.*, *Appl. Therm. Eng.* (2009) **29**, 418.
19. Kim, I. D., *et al.*, *Nano Lett.* (2006) **6**, 2009.
20. Huang, C. B., *et al.*, *Nanotechnology* (2006) **17**, 1558.
21. Ding, B., *et al.*, *Nanotechnology* (2006) **17**, 3685.
22. Wang, X. F., *et al.*, *Nanotechnology* (2010) **21**, 055502.
23. Ding, B., *et al.*, *Thin Solid Films* (2008) **516**, 2495.
24. Parajuli, D. C., *et al.*, *ACS Appl. Mater. Interf.* (2009) **1**, 750.
25. Janata, J., *et al.*, *Anal. Chem.* (1994) **66**, R207.
26. Crooks, R. M., and Ricco, A. J., *Acc. Chem. Res.* (1998) **31**, 219.
27. Li, Y., *et al.*, *Sens. Actuators, B* (2010) **145**, 516.
28. He, X. L., *et al.*, *Sens. Actuators, B* (2010) **145**, 674.
29. Marx, K. A., *Biomacromolecules* (2003) **4**, 1099.
30. Ding, B., *et al.*, *Sens. Actuators, B* (2004) **101**, 373.
31. Wang, X. F., *et al.*, *Int. J. Nonlinear Sci. Numer. Simul.* (2010) **11**, 517.
32. Ding, B., *et al.*, *Sens. Actuators, B* (2005) **106**, 477.
33. Ding, B., *et al.*, *Nanotechnology at the Leading Edge, Nova Science Publishers, New York* (2006), 1.
34. Wang, X. F., *et al.*, *Sens. Actuators, B* (2010) **144**, 11.
35. Ding, B., *et al.*, *Sensors* (2009) **9**, 1609.
36. Wang, Y., *et al.*, *Sensors* (2009) **9**, 6752.
37. Choi, S. H., *et al.*, *ACS Nano* (2009) **3**, 2623.
38. Zhang, Z. Y., *et al.*, *J. Phys. Chem. C* (2009) **113**, 19397.
39. Qi, Q., *et al.*, *Sens. Actuators, B* (2009) **137**, 471.
40. Li, Z. Y., *et al.*, *J. Am. Chem. Soc.* (2008) **130**, 5036.
41. Zhang, G., and Liu, M. L., *Sens. Actuators, B* (2000) **69**, 144.
42. Liu, Y., *et al.*, *Adv. Mater.* (2004) **16**, 353.
43. Qi, Q., *et al.*, *Sens. Actuators, B* (2009) **141**, 174.
44. Zheng, W., *et al.*, *J. Am. Ceram. Soc.* (2010) **93**, 15.
45. Song, X., *et al.*, *Nanotechnology* (2009) **20**, 075501.
46. Zhang, Y., *et al.*, *Sens. Actuators, B* (2008) **13**, 67.
47. Song, X. F., *et al.*, *Appl. Surf. Sci.* (2009) **255**, 7343.
48. Song, X. F., *et al.*, *Sens. Actuators, B* (2009) **138**, 368.
49. Stutzmann, N., *et al.*, *Science* (2003) **299**, 1881.
50. Liu, H. Q., *et al.*, *Nano Lett.* (2004) **4**, 671.
51. Gao, Y., *et al.*, *J. Phys. Chem. C* (2008) **112**, 8215.
52. Ji, S. Z., *et al.*, *Sens. Actuators, B* (2008) **133**, 644.
53. Bishop-Haynes, A., and Gouma, P., *Mater. Manuf. Process.* (2007) **22**, 764.
54. Pinto, N. J., *et al.*, *Sens. Actuators, B* (2008) **129**, 621.
55. Manesh, K. M., *et al.*, *IEEE Trans. Nanotechnol.* (2007) **6**, 513.
56. Aussawasathien, D., *et al.*, *Synth. Met.* (2008) **158**, 259.
57. Lala, N. L., *et al.*, *Sensors* (2009) **9**, 86.
58. Haglund, R. F., *et al.*, *Opt. Lett.* (1993) **18**, 373.
59. Hu, M. S., *et al.*, *Nat. Mater.* (2006) **5**, 102.
60. Shi, W., *et al.*, *J. Colloid Interface Sci.* (2009) **340**, 291.
61. Wu, H., *et al.*, *Adv. Mater.* (2009) **21**, 227.
62. Wang, X. Y., *et al.*, *Nano Lett.* (2002) **2**, 1273.
63. Wang, X. Y., *et al.*, *Nano Lett.* (2004) **4**, 331.
64. Chae, S. K., *et al.*, *Adv. Mater.* (2007) **19**, 521.
65. Luoh, R., and Hahn, H. T., *Composites Sci. Technol.* (2006) **66**, 2436.
66. Newman, J. D., and Turner, A. P. F., *Biosens. Bioelectron.* (2005) **20**, 2435.
67. Abdellatif, M. S., and Guilbault, G. G., *Anal. Chem.* (1988) **60**, 2671.
68. Bossi, A., *et al.*, *J. Chromatogr.* (2000) **892**, 143.
69. Ghica, M. E., and Brett, C. M. A., *Anal. Lett.* (2005) **38**, 907.
70. Wang, Z. G., *et al.*, *J. Phys. Chem. C* (2009) **113**, 2955.
71. Ren, G. L., *et al.*, *React. Funct. Polym.* (2006) **66**, 1559.
72. Liu, H. Y., *et al.*, *Electroanalysis* (2006) **18**, 2055.
73. Liu, Y., *et al.*, *Biosens. Bioelectron.* (2009) **24**, 3329.
74. Wang, W., *et al.*, *Biosens. Bioelectron.* (2009) **25**, 708.
75. Wang, W., *et al.*, *Electrochem. Commun.* (2009) **11**, 1811.
76. Manesh, K. M., *et al.*, *Anal. Biochem.* (2007) **360**, 189.
77. Ding, Y., *et al.*, *Biosens. Bioelectron.* (2010) **25**, 2009.
78. Sawicka, K., *et al.*, *Sens. Actuators, B* (2005) **108**, 585.
79. Lin, J. Y., *et al.*, *ACS Appl. Mater. Interf.* (2010) **2**, 521.
80. Wang, M. R., *et al.*, *Phys. Rev. E* (2007) **75**, 036702.
81. Zhang, Y., *et al.*, *Sens. Actuators, B* (2010) **144**, 43.
82. Agarwal, S., *et al.*, *Adv. Funct. Mater.* (2009) **19**, 2863.
83. Park, J. Y., *et al.*, *J. Am. Ceram. Soc.* (2009) **92**, 2551.
84. Wang, Y., *et al.*, *Electroanalysis* (2009) **21**, 1432.
85. Sokolov, A. N., *et al.*, *Mater. Today* (2009) **12**, 12.
86. Wang, M. R., and Pan, N., *Mater. Sci. Eng. R-Rep.* (2008) **63**, 1.
87. Koombhongse, S., *et al.*, *J. Polym. Sci. Pt. B-Polym. Phys.* (2001) **39**, 2598.
88. Landau, O., *et al.*, *Chem. Mater.* (2009) **21**, 9.
89. Zhang, H. N., *et al.*, *Talanta* (2009) **79**, 953.
90. Wang, Y., *et al.*, *IEEE Sens. J.* (2007) **7**, 1347.
91. Yang, A., *et al.*, *Appl. Phys. Lett.* (2007) **91**, 2783479.
92. Wang, Z. X., and Liu, L., *Mater. Lett.* (2009) **63**, 917.
93. Zheng, W., *et al.*, *Mater. Res. Bull.* (2009) **44**, 1432.
94. Wu, W. Y., *et al.*, *Nanoscale Res. Lett.* (2009) **4**, 513.
95. Wang, J. X., *et al.*, *Mater. Lett.* (2009) **63**, 1750.
96. Zheng, W., *et al.*, *J. Colloid Interface Sci.* (2009) **338**, 366.
97. Wang, G., *et al.*, *J. Phys. Chem. B* (2006) **110**, 23777.
98. Sahner, K., *et al.*, *Sensors* (2007) **7**, 1871.
99. Li, P., *et al.*, *Sens. Actuators, B* (2009) **141**, 390.
100. Kessick, R., and Tepper, G., *Sens. Actuators, B* (2006) **117**, 205.
101. Yang, M., *et al.*, *Appl. Phys. A-Mater. Sci. Process.* (2007) **89**, 427.